Photochemical & Photobiological Sciences

Accepted Manuscript

This is an *Accepted Manuscript*, which has been through the Royal Society of Chemistry peer review process and has been accepted for publication.

Accepted Manuscripts are published online shortly after acceptance, before technical editing, formatting and proof reading. Using this free service, authors can make their results available to the community, in citable form, before we publish the edited article. We will replace this *Accepted Manuscript* with the edited and formatted *Advance Article* as soon as it is available.

You can find more information about *Accepted Manuscripts* in the Information for Authors.

Please note that technical editing may introduce minor changes to the text and/or graphics, which may alter content. The journal's standard Terms & Conditions and the Ethical guidelines still apply. In no event shall the Royal Society of Chemistry be held responsible for any errors or omissions in this *Accepted Manuscript* or any consequences arising from the use of any information it contains.

ROYAL SOCIETY OF CHEMISTRY

www.rsc.org/pps

Cite this: DOI: 10.1039/c0xx00000x

www.rsc.org/xxxxxx

ARTICLE TYPE

Effect of amphiphilic polymer on the association, morphology and photophysical properties of hypocrellin coordination polymer/fullerene assemblies

Zhize Ou,*[a] Guixia Liu,[a] Yunyan Gao,*[a] Shayu Li,[b] Huizhen Li,[a] Yi Li,[c] Xuesong Wang,[c] Guoqiang Yang[b], Xin Wang[a]

Received (in XXX, XXX) Xth XXXXXXXXX 20XX, Accepted Xth XXXXXXXXX 20XX
DOI: 10.1039/b000000x

The Yttrium coordination polymer of pyrene modified hypocrellin A (Y^{3+}-PyrHA) is synthesized and characterized. The methoxydiglycol malonate modified fullerene can be included in the cavity of Y^{3+}-PyrHA in organic solution and buffer solution containing amphiphilic polymer, such as polyvinyl pyrrolidone (PVP), Pluronic F127 and P123. The interaction between amphiphilic polymer and Y^{3+}-PyrHA plays an important role in controlling the size and morphology of Y^{3+}-PyrHA/fullerene. TEM images of Y^{3+}-PyrHA/fullerene in 1% F127 and P123 show nanoparticles in the size range 10–60 nm, while TEM images of Y^{3+}-PyrHA/fullerene in 1% PVP display large-scale aggregation. Singlet oxygen is generated by irradiation of the polymer solution of Y^{3+}-PyrHA/fullerene in the presence of oxygen. The electron paramagnetic resonance (EPR) spin trapping and 9,10-Dimethoxyanthracene-2-sulfonic acid sodium salt (MAS) photooxidation results suggest that in 1% P123 solution Y^{3+}-PyrHA/fullerene exhibits higher singlet oxygen quantum yield than Y^{3+}-PyrHA and corresponding fullerene.

Introduction

Research in the areas of coordination polymers has been undertaken for over fifty years due to the limitless choices of metal and organic building blocks.[1] The tunable nature of coordination polymers has allowed them to be exploited for a broad range of applications, including heterogeneous catalysis, porous membranes, thin-film devices, biomedical imaging and biosensing, and controlled drug release.[2] Recently, downsizing of coordination polymer crystals/particles into the nanometer regime has gradually attracted much attention.[3] The nanoscale coordination polymers exhibit a high level of structural tailorability, including size- and morphology-dependent properties, and the functional species such as drugs, dyes, light emitters, magnetic molecules and explosives, can be deliberately encapsulated into these network structures.[4-6]

Amphiphilic polymers, such as polyvynyl pyrolidone (PVP) and polyethylene glycol (PEG), have been used as stabilizer for controlling the size of coordination polymer and protecting the coordination polymer nanoparticles from aggregation.[7] The weak interaction between organic polymer and coordination polymer may facilitate the formation of supramolecular assembly. Coacervate core micelles can be formed by a coordination polymer and a diblock copolymer through electrostatic interaction.[8] Pluronic polymer F127, composed of hydrophilic poly(ethylene oxide) (PEO) blocks and hydrophobic poly(propylene oxide) (PPO) blocks, with the structure of PEO_{100}-PPO_{65}-PEO_{100}, can separate the metal-oligochitosan (CTS) network and the PEO blocks may participate in the coordination to form a "double host metal-drug" system.[9] Organic polymer can also act as reactant in preparation of coordination polymers. Nanoscale Prussian Blue (PB) are synthesized by using $K_3[Fe(CN)_6]$ as a single-source precursor and PVP as a capping and reducing agent, and the size or morphology of PB can be tuned by adjusting the feed ratio of $K_3[Fe(CN)_6]$ to PVP.[10]

Fullerenes have attracted a great deal of interest owing to its unique photophysical and biological activities.[11] However, fullerene molecules tend to aggregate in aqueous solutions, and the life time of the triplet state decreases dramatically due to the excitation quenching processes caused by fullerene-fullerene interactions.[12] The reduced triplet lifetime of fullerene clusters preclude most biological applications in physiological media, including photocleavage of DNA, antiviral effect, and use as photosensitizers for photodynamic therapy (PDT).[13] To solve this problem, one important approach is hybridization of fullerenes with polymer materials, such as conjugation with water-soluble polymers,[14] assembling with coordination polymer,[15,16] encapsulation within block polymer micelles.[17] It has been reported that nanoparticles within the 2–100 nm size range are found to alter signalling processes essential for basic cell functions (including cell death).[18] The nanoparticles of fullerene/polymer hybrids can easily enter into cells and hence have been developed for biomedical uses.[19]

Preparation of stable fullerene nanoparticle with narrow size distribution and homogeneous morphology is of immense importance.[20] Hypocrellin and its coordination polymers can form supramolecular assembly with fullerene, and the resulting

assemblies possess moderate solubility in polar solvent and display photodynamic activities.[16,21] However, the nanostructures of these assemblies are not investigated in detail. In this study, Yttrium coordination polymer of pyrene modified hypocrellin A (Y^{3+}-PyrHA) is prepared. Pyrene could form complex with fullerene,[22] which would facilitate the association between Y^{3+}-PyrHA and fullerenes. Pluronic polymers, including F127 and P123 (PEO_{19}-PPO_{69}-PEO_{19}), and PVP are selected to control the nanostructure and optimize the photodynamic properties of Y^{3+}-PyrHA/fullerene complex. The reasons to choose these polymers are as follows. First, Pluronic polymers and PVP can be used as stabilizer for nanoscale coordination polymers (NCPs)[9,10] and as excipients for drug-loaded NCPs due to their low toxicity.[23] Second, PVP and Pluronic polymers can form complex with fullerene derivatives and keep them in a soluble state.[20,24] Third, different from the single component PVP polymer, the triblock copolymers F127 and P123 can self-assemble into core-shell micelles and incorporate poorly water-soluble drugs into the PPO hydrophobic core.[25] The binding behavior in Y^{3+}-PyrHA/fullerene assembly and the morphology and photophysical properties of Y^{3+}-PyrHA/fullerene nanoparticle are investigated in the presence of PVP, Pluronic F127 and P123.

Experimental section

Chemicals and instruments

N,N'-Dimethyl formamide (DMF), dimethylsulfoxide (DMSO), 1-pyrenebutyric acid, mercaptoethanol and $YCl_3.6H_2O$ were purchased from Acros Organics. N-Ethyl-N'-(3-dimethylaminopropyl)carbodimide hydrochloride (EDC), Pluronic® F127, Pluronic® P123, Polyvinyl pyrrolidone K30 (PVP), 4-dimethylaminopyridine (DMAP), 9,10-Dimethoxyanthracene-2-sulfonic acid sodium salt (MAS), fullerene C_{60} and C_{70} were purchased from Sigma-Aldrich Company. Hypocrellin A (HA) was isolated from the fungus sacs of *Hypocrella bambusae* and recrystallized twice from acetone before use. Methoxydiglycol malonate modified fullerene C_{60} (MMC_{60}) and C_{70} (MMC_{70}) were synthesized according to literature procedures (Fig. 1).[26] DMF and DMSO were dried over CaH_2 and distilled prior to use. Anhydrous ethanol and other chemicals of analytical grade were obtained from Beijing Chemical Plant and redistilled before use.

Hydrodynamic radius (Rh) and polydispersity index (PDI) of nanoparticles were measured using dynamic light scattering (DLS) (Malvern company, UK; Zatasizer Nano ZS). ^{1}H NMR and ^{13}C NMR spectra were obtained using a Bruke-400 NMR instrument. The nanoparticles were imaged using TEM (JEOL, Ltd., Japan; JEOL-2010) at an acceleration voltage of 120 KV.

Synthesis of di-(mercaptoethanol) substituted HA (DEHA) (2)

Compound 1 (HA) (0.2 g, 0.37 mmol) was put into 400 mL of ethanol-H_2O (1/3, v/v) solution of 0.14 % NaOH (0.56 g, 14 mmol), and stirred at room temperature for 30 min. Mercaptoethanol (2.228 g, 28 mmol) was added into the mixture and irradiated with a medium pressure sodium lamp (> 470 nm) at 15 ^{o}C for 4 h. The reaction solution was bubbled with air (10 mL.min^{-1}). After irradiation, the solution was acidified with 10% hydrochloric acid and extracted with chloroform. The mixture

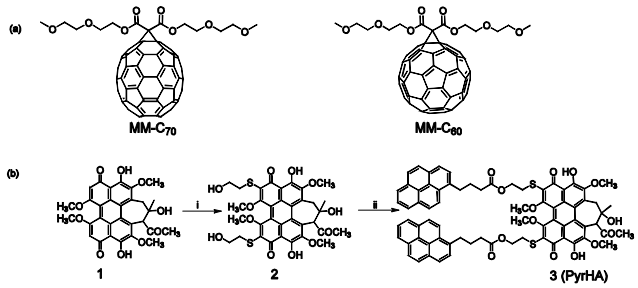

Fig. 1 (a) Chemical structure of MMC_{70} and MMC_{60}. (b) Synthesis of pyrene modified HA (PyrHA). Reagents and conditions: (i) $HSCH_2CH_2OH$, $h\nu$ > 470 nm, pH = 10; (ii) 1-pyrenebutyric acid, EDC, DMAP.

was isolated by thin layer chromatography (TLC) on silica gel with chloroform-ethyl acetate 1:1 mixture as eluent, and 0.18 g of di(mercaptoethanol) substituted HA (DEHA) was obtained (yield: 70 %). ^{1}H NMR (400 MHz, $CDCl_3$): 15.90 (s, 2H, exchanged with D_2O, phenolic OH), 3.75-4.20 (m, 19H), 3.12-3.34 (m, 4H), 2.38 (s, 3H), 1.93 (s, 3H), 1.86 (s, 3H). FAB-MS ([M-H]$^-$): 698.

Synthesis of pyrene modified HA (PyrHA) (3)

Compound 2 (0.050 g, 0.071 mmol) and 1-pyrenebutyric acid (0.050 g, 0.17 mmol) were dissolved in 15 mL DMF and then 4-dimethylaminopyridine (DMAP, 0.050 g, 0.41 mmol) and 1-(3-Dimethylaminopropyl)-3-ethylcarbodiimide (EDC, 0.110 g, 0.573 mmol) were added. After stirring for 48 h at room temperature, the reaction solution was evaporated under vacuum. The crude product was purified by TLC on silica gel with chloroform-ethyl acetate 5:1 mixture as eluent, and 0.056 g of pyrene modified HA (PyrHA) was obtained (yield 74 %). ^{1}H NMR (400 MHz, $CDCl_3$): 15.840 (s, 2H, exchanged with D_2O, phenolic OH), 8.18 (d, 1H), 8.11 (d, 2H), 8.07 (d, 1H), 8.03 (d, 2H) , 7.97 (d, 2H), 7.75 (d, 1H), 4.27 (m, 4H), 3.65-4.2 (m, 14H), 3.39 (m, 3H), 3.26 (m, 6H), 3.07 (d, 1H), 2.35 (m, 4H), 2.31 (s, 2H), 2.09 (s, 5H), 1.88 (s, 3H). MALDI-TOF: 1261.6 [M+Na$^+$], calcd for $C_{74}H_{62}O_{14}S_2Na$ 1261.4.

Synthesis of Y^{3+} coordination polymer of PyrHA (Y^{3+}-PyrHA)

A solution of YCl_3 (0.5 mM) was added dropwise to equal volume of PyrHA (1 mM) in ethanol. The resulting solution was stirred overnight at room temperature in the dark. After the solvent was evaporated completely, the residue was redissolved in ethanol and dialyzed against anhydrous ethanol employing a spectrapor membrane with a molecular weight cutoff of > 5,000. The remaining solution within the dialysis bag was dried under high vacuum, and the desired complex was obtained. ^{1}H NMR (400 MHz, DMSO-d6): 15.958 (s, 2H, exchanged with D_2O, phenolic OH), 8.116-8.304 (m, 3H), 7.867-8.085 (m, 5H), 7.618-7.808 (m, 1H), 4.075-4.356 (m, 2H), 4.058-3.804 (m, 6H), 3.804-3.688 (m, 3H), 3.673-3.595 (m, 2H), 3.583-3.529 (m, 2H), 3.529-3.461 (m, 4H), 3.454-3.408 (m, 5H), 3.199-2.978 (m, 5H), 2.391-1.975 (m, 8H), 1.944-1.625 (m, 8H).

Measurements of spectral properties

Steady state absorption and fluorescence spectra were recorded with a Hitachi UV-3010 UV-vis spectrophotometer and Hitachi F-4600 spectrometer, respectively. The fluorescence experiments were carried out in a 5 mm × 5 mm cuvette.

Nanosecond transient absorption spectra were performed on a LP-920 pump-probe spectroscopic setup (Edinburgh). The excited source was a Nd:YAG laser (355 nm); the probe light source was a pulse-xenon lamp. The signals were detected by Edinburgh analytical instruments (LP900) and recorded on a Tektronix TDS 3012B oscilloscope and a computer.[27]

EPR spectra were obtained using a Bruker ESP-300E spectrometer operating at room temperature, and the operating conditions were as following: microwave bridge, X-band with 100 Hz field modulation; sweep width, 200 G; receiver gain, 1×10^5; microwave power, 5 mW. Samples were injected into the specially made quartz capillaries for EPR analyses, purged with argon, air or oxygen for 30 min in the dark, respectively, according to the experimental requirements, and illuminated directly in the cavity of the EPR spectrometer with a Nd:YAG laser (532 nm) except as noted elsewhere.

UV-vis titrations

The titrations were performed by adding the required volumes of a solution of fullerene derivative (1 mM) in toluene to 3 mL of the DMSO-toluene solution of Y^{3+}-PyrHA (15 μM), by using a reference solution with the same concentration of fullerene.

Fluorescence titration

The titrations were performed by adding the required volumes of a solution of fullerene (1 mM) into the solution of Y^{3+}-PyrHA (2 μM). The fluorescence intensity of Y^{3+}-PyrHA decreased with increasing fullerene concentration. In order to eliminate inner-filter effect, all the fluorescence intensities of Y^{3+}-PyrHA were corrected according to eqn (1):[28]

$$F_{real} = F_{measured} \times 10^{[(A_{ex}+A_{em})/2]} \quad (1)$$

where F_{real} and $F_{measured}$ were the corrected and observed fluorescence of Y^{3+}-PyrHA, A_{ex} and A_{em} were the absorbance of fullerene at the excitation (347 nm) and emission (380 nm) wavelengths of Y^{3+}-PyrHA, respectively. The absorption coefficients (ε) at 347 nm for MMC_{60} (lgε = 4.38) and MMC_{70} (logε =4.56), and at 380 nm for MMC_{60} (logε = 3.97) and MMC_{70} (logε =4.67) were used for the calculation. The association constant (K_a) of the formed Y^{3+}-PyrHA/fullerene complex could be determined using the nonlinear least squares method according to the curve fitting.[21,29]

Results and discussion

Synthesis of Y^{3+} coordination polymer of PyrHA

The pH value of solution is important for the yield of the reaction between thiol compounds and hypocrellins.[30] The pk_a of mercaptoethanol is 9.72,[31] and the pH value of reaction solution can be conveniently modulated to 10 by addition of mercaptoethanol and NaOH with the molar ratio of 2:1. 5,8-di-mercaptoethanol-HA (DEHA) is obtained as the main product when the reaction is carried out in the presence of oxygen. The pyrene modified HA (PyrHA) is further synthesized by esterification of DEHA with 1-pyrenebutyric acid by using EDC as coupling reagents.[32]

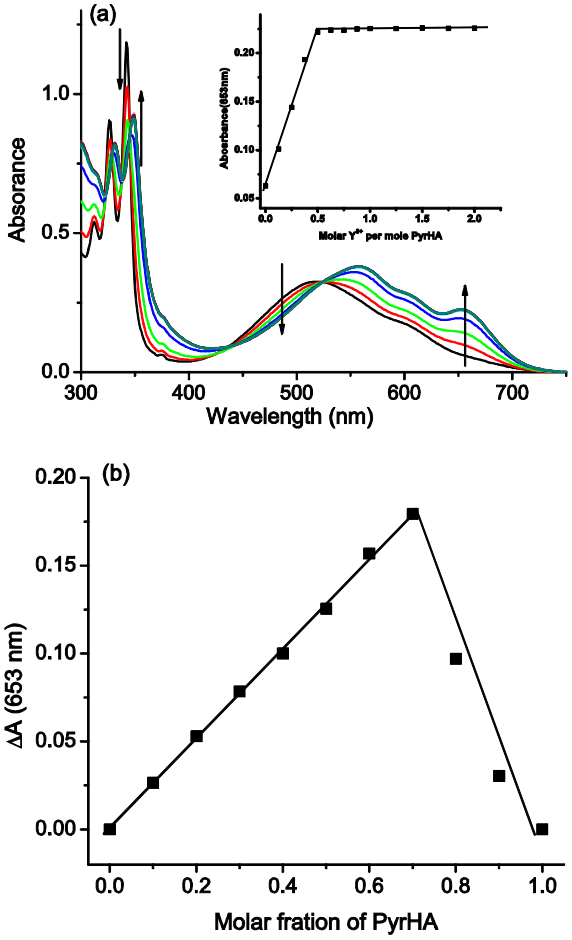

Fig. 2 (a) Absorption spectral changes of PyrHA in ethanol upon addition of Y^{3+}. [PryHA] = 20 μM. [Y^{3+}] = 0, 2.5, 5, 7.5, 10, 12.5, 15, 17.5, 20, 25, 30, 35, 40 μM. (b) Job's plot for the Y^{3+}−PyrHA in ethanol obtained by plotting the absorbance differences (ΔA) at 653 nm ([PyrHA] + [Y^{3+}] = 40 μM). Inset: Molar ratio plot for Y^{3+}-PyrHA obtained by plotting the absorbance at 653 nm as a function of the molar ratio of Y^{3+} to PyrHA.

In ethanol solution, PyrHA exhibits four absorption peaks at 312, 326, 342 and 514 nm, respectively. The absorption peaks at 312, 326 and 342 nm can be assigned to the π-π* transitions located on the pyrene subunits, and the absorption peak at 514 nm is attributed to π-π* transition located on the HA subunit. Upon addition of Y^{3+}, these peaks are red-shifted to 314, 331, 348, and 555 nm, respectively, with a new peak appearing at 653 nm (Fig. 2a). Remarkable changes in the absorption spectra indicate that Y^{3+} can strongly chelate with PyrHA. During the entire titration processes, one set of isosbestic points at 322, 329, 346, 440 and 524 nm is observed within the spectral region (250−750 nm) under study, indicating that only one form of complex is produced in the system.

The stoichiometry of the complex is determined by both molar ratio and continuous variation methods.[33] For the molar ratio method, a series of ethanol solutions is prepared in which the

concentration of PyrHA is held constant (20 μM), while that of the Y^{3+} is varied. The absorbance at 653 nm is plotted against the molar ratio of [Y^{3+}]/[PyrHA] (Fig. 2a, inset). Two straight lines

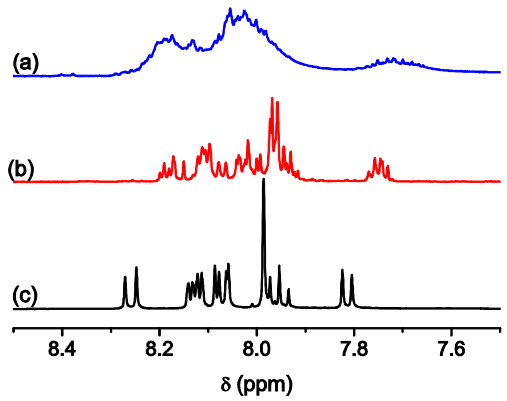

Fig. 3 ^{1}H NMR spectra of (a) Y^{3+}-PyrHA and (b) PyrHA in DMSO-d_6, and (c) 1-pyrenebutyric acid in $CDCl_3$ in the range of 8.5-7.5 ppm. Concentrations are about 5 mM.

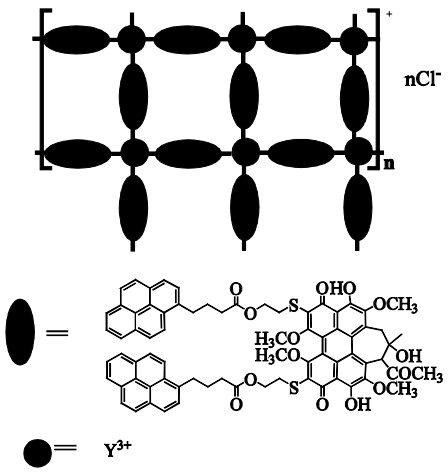

Fig. 4 Proposed 2-D structure for Y^{3+}-PyrHA

of different slops can be derived from the plot, and the extrapolated intersection occurs at a mole ratio of 0.5 ([Y^{3+}]/[PyrHA]), corresponding to the ratio of Y^{3+} to PyrHA in the complex. For the continuous variation method, the total concentration of Y^{3+} and PyrHA is kept constant (40 μM), while the molar fractions of Y^{3+} in the mixed solutions continuously varied. The absorbance differences (ΔA) between the mixed solutions and the neat PyrHA solution are plotted against the molar fraction of PyrHA. As shown in Fig. 2b, the maximum ΔA occurs at the molar fraction of 0.66, supporting the 1:2 molar ratio of Y^{3+} and PyrHA in the complex, too.

Complexation also gives rise to significant changes in ^{1}H NMR and IR spectra of PyrHA. The ^{1}H NMR signals of the pyrene moiety in Y^{3+}-PyrHA are significantly broadened when compared with the corresponding signals in PyrHA and 1-pyrenebutyric acid (Fig. 3). This broadening is likely due to chemical exchange caused by aggregation-disaggregation equilibrium of Y^{3+}-PyrHA in solution.[34] The upfield shifts in pyrene ring protons can be attributed to the intramolecular stacking in Y^{3+}-PyrHA.[35] The ^{1}H NMR signal of the phenolic hydroxyl group of PyrHA shifts downfield from δ 15.840 to 16.958 upon complexation. The IR absorption band for the C=O stretching vibration of the quinonoid

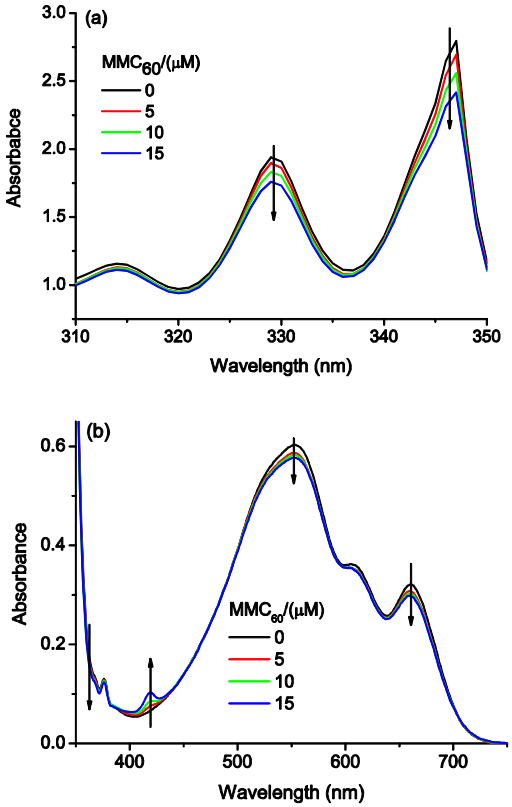

Fig. 5 UV-vis spectral changes of Y^{3+}-PyrHA (15 μM) in the range of (a) 310~350 and (b) 350~750 nm in DMSO-toluene solution (4/1, v/v) upon addition of MMC_{60}.

carbonyl group in PyrHA shifts from 1652 cm^{-1} to 1640 cm^{-1} in the complex Y^{3+}-PyrHA. These results suggest that phenolic hydroxyl and quinonoid carbonyl groups in PyrHA participate in coordination.

Taking the fact that the coordination number of the Y^{3+} can be up to eight in coordination polymer and also taking all the above-mentioned findings into consideration, the structure of Y^{3+}-PyrHA is proposed to be a 2-D coordination polymer (Fig. 4), similar to that of Y^{3+} coordination polymer of tryptamine modified HA.[21] Addition of $AgNO_3$ to the aqueous solution of Y^{3+}-PyrHA leads to the precipitation of AgCl, suggesting that Cl^- is the counterion in the complex. Some fragments of Y^{3+}-PyrHA coordination polymer could be observed in MALDI-TOF mass spectrum (Fig. S1), further confirming the proposed structure of Y^{3+}-PyrHA.

Interaction between fullerenes and Y^{3+}-PyrHA

The interaction between fullerene derivatives and Y^{3+}-PyrHA is investigated by UV-vis absorption. Upon addition of MMC_{60}, the absorption bands at 314, 329, 347, 552, 610 and 660 nm decrease gradually, and a new shoulder band at 420 nm appears (Fig. 5a, b). Meanwhile, two clear isosbestic points are observed at 388 and 442 nm. Similarly, addition of MMC_{70} into the solution of

Y^{3+}-PyrHA also leads to decrease in the absorption peaks of Y^{3+}-PyrHA (data not shown). On the other hand, addition of MMC_{60} or MMC_{70} leads to negligible changes of the absorption peaks of PyrHA, suggesting weak interaction between PyrHA and MMC_{60}. These results suggest Y^{3+}-PyrHA can form stable complex with

Table 1 Apparent 1:1 association constants (K_a) ($\times 10^5$ M^{-1}) for the complexation of fullerene derivatives with Y^{3+}-PyrHA under different solution conditions

Compound	DMSO-toluene (4/1, v/v)	P123		F127		PVP	
		0.01%	1%	0.01%	1%	0.05%	1%
MMC_{60}	N.D[a]	1.37	2.11	0.91	0.90	0.41	4.6
MMC_{70}	N.D[a]	0.92	1.41	4.22	4.28	1.71	2.88

[a]not detected.

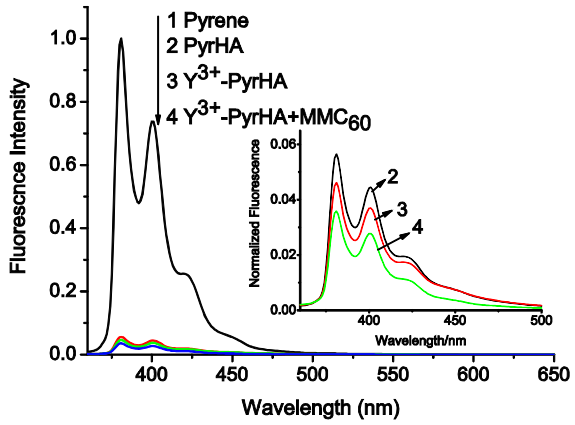

Fig. 6 Fluorescence emission spectra of (1) Pyrene (40 μM), (2) PyrHA (20 μM), (3) Y^{3+}-PyrHA (10 μM), and (4) Y^{3+}-PyrHA (10 μM) + MMC_{60} (10 μM) in DMSO-toluene solution (4/1, v/v). Inset: emission from 360 to 500 nm magnified (λ_{ex} = 347 nm).

MMC_{60} and MMC_{70}, which can be due to the synergy effect of the PyrHA unit in the coordination polymer.[36]

Along with the UV−vis spectral changes, a decrease in the fluorescence intensity of Y^{3+}-PyrHA at 381 and 400 nm (assigned to the pyrene moiety) is also observed upon addition of MMC_{60} or MMC_{70}. The fluorescence intensity of pyrene in PyrHA is much lower than that of free 1-pyrenebutyric acid at the same concentration of pyrene unit (Fig. 6), which can be attributed to electron transfer between excited pyrene and hypocrellin group. Free energy change (ΔG) involving electron transfer from singlet excited state of pyrene unit to the ground state of hypocrellin moiety is a thermodynamic favorable process (ΔG = -1.10 eV), calculated by Rehm-Weller equation (eqn (2)), using oxidation potential of pyrene (1.25 V vs SCE),[37] first reduction potential of thiol substituted hypocrellin (-0.98 V vs SCE)[20] and singlet state energy of pyrene (3.33 ev).[38] The reduction potential of quinone is more positive after coordination with Y^{3+},[21,39] which may facilitate electron transfer from singlet state of pyrene moiety to HA moiety in Y^{3+}-PyrHA. As a result, Y^{3+}-PyrHA has lower fluorescence than that of PyrHA.

$$\Delta G = E_{ox(donor)} - E_{Red(acceptor)} - E_0 \quad (2)$$

The fluorescence at 381 and 400 nm of the pyrene moiety in Y^{3+}-PyrHA is further quenched by MMC_{60}. On the other hand, in the presence of Y^{3+}-PyrHA, the fluorescence of MMC_{60} at near 700 nm increases slightly (Fig. S2). The above results suggest energy transfer from pyrene to MMC_{60} may be the possible pathway for fluorescence quenching by MMC_{60} (Fig. S2).[40]

To quantitatively assess the inclusion complexation behavior of Y^{3+}-PyrHA with MMC_{60} and MMC_{70}, fluorescence titrations

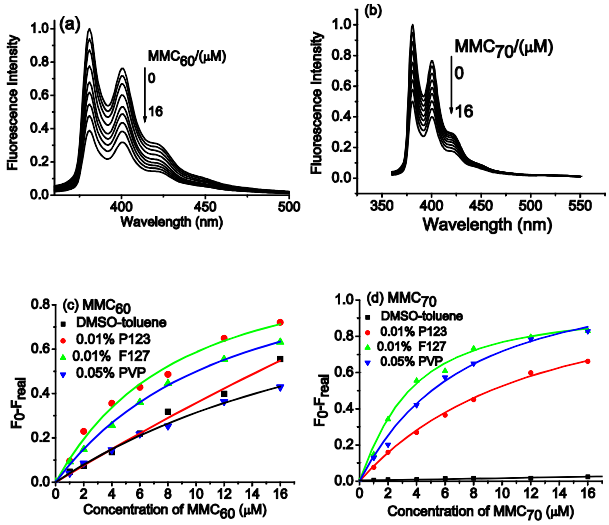

Fig. 7 Fluorescence emission spectra of Y^{3+}-PyrHA (2.0 μM) in DMSO-toluene solution (4/1, v/v) containing different concentration of (a) MMC_{60} and (b) MMC_{70} (λ_{ex} = 347 nm). Differential fluorescence intensity of Y^{3+}-PyrHA upon addition of (c) MMC_{60} and (d) MMC_{70} used to calculate K_a by nonlinear least-square curve fitting analysis in DMSO-toluene, 0.05% PVP, 0.01% F123 and 0.01% F127 solution. 5 mm × 5 mm cuvette is used for fluorescent measurement.

of Y^{3+}-PyrHA with MMC_{60} or MMC_{70} are performed in DMSO-toluene solution (4/1, v/v) (Fig.7a and b). MMC_{60} and MMC_{70} can absorb significantly both the excitation and the emission light of pyrene, which will cause a significant decrease of the measured intensity due to "inner-filter effect"[28]. To reduce the inner effect, the cuvette with an optical path of 5 mm is used in our experiments. The measured fluorescence intensities are further calibrated according to eqn(1). Assuming 1:1 inclusion complexation stoichiometry between Y^{3+}-PyrHA and fullerene derivatives, the association constants (K_a) could be calculated by analyzing the sequential changes in fluorescence intensity ($\Delta F = F_0 - F_{real}$) of Y^{3+}-PyrHA at various concentrations of fullerenes by using a nonlinear least-squares curve-fitting method (Fig. 7c and d), where F_0 is the fluorescence of Y^{3+}-PyrHA in the absence of fullerene. The fits for association of MMC_{60}/MMC_{70} with Y^{3+}-PyrHA in DMSO-toluene are straight lines, suggesting that the interaction between MMC_{60}/MMC_{70} and Y^{3+}-PyrHA is very weak (Table 1). It has been reported that hypocrellin A and pyrene weakly interact with C_{70}.[21,41]

To investigate the influence of amphiphilic polymer on the complexing behavior of Y^{3+}-PyrHA with fullerene derivatives, fluorescence titration is performed in F127, P123 and PVP solution, respectively. The plot of ΔF as a function of fullerene

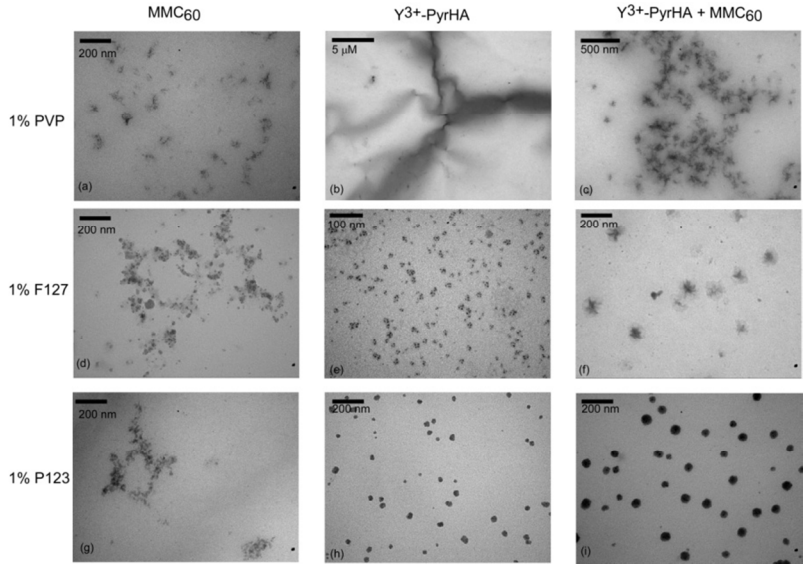

Fig. 8 TEM images of MMC_{60} (a, d, g), Y^{3+}-PyrHA (b, e, h), and Y^{3+}-PyrHA/MMC_{60} (c, f, i) in buffer solution (HEPES, 10 mM, pH 7.4) containing 1% PVP, 1% F127 or 1% P123. [MMC_{60}] = [Y^{3+}-PyrHA] = 50 μM.

concentration gives an excellent fit ($R^2 > 0.994$), verifying the validity of the 1:1 complex stoichiometry assumed (Fig. 7c and d). It is worth noting that the ratio given above does not mean that fullerene and Y^{3+}-PyrHA form individual 1:1 complexes in aqueous solution. This notion describes the number of the components present within the polymeric assembled fullerene and Y^{3+}-PyrHA. As a result, the association constant could be termed as apparent 1:1 association constant. In repeated measurements, the association constant values are reproducible within an error of ± 5%. The association constants values obtained for Y^{3+}-PyrHA/fullerene derivatives are summarized in Table 1. The nature of capturing fullerene by Y^{3+}-PyrHA may be due to π-π stacking interaction between PyrHA and fullerene, like the case of the nonconvalent binding of fullerenes by aromatic components such as porphyrin and calixarenes.[42]

In all amphiphilic polymer solution, the association constant between Y^{3+}-PyrHA and fullerene derivatives increase dramatically (Table 1), which can be attributed to the chemical microenvironments provided by amphiphilic polymers.[43] Pluronic block polymer P123 and F127 can self-assemble into micelles under our experimental condition, due to their low critical micelle concentration (~10^{-6} M).[44] Y^{3+}-PyrHA, bearing lipophilic side chain, and fullerene derivatives are physically entrapped in the hydrophobic core of a micelle, which may facilitate the interaction between Y^{3+}-PyrHA and fullerene derivative due to the high local concentration. PVP is remarkable for its capacity to interact with a wide variety of hydrophilic and hydrophobic pharmaceutical agents and enhance their water solubility.[45] As a result, Y^{3+}-PyrHA and fullerene derivative may simultaneously interact with PVP and form supramolecular system. The association constants between Y^{3+}-PyrHA and fullerene derivative increase when the concentration of amphiphilic polymer increases from 0.01% to 1% (Table 1).

Transmission Electron Microscopy (TEM)

We have previously shown that in ethanol solution, the morphology of MMC_{60} changed greatly when forming complex with Y^{3+} coordination polymer of tryptamine modified HA (Y^{3+}-DTrpHA).[21] In this work, the influence of polymers, including 1% PVP, 1% F127 and 1% P123 aqueous solution, on the morphology of Y^{3+}-PyrHA/MMC_{60} is investigated and the results are shown in Fig. 8. The TEM image of MMC_{60} shows cluster–cluster aggregation in 1% PVP, 1% F127 and 1% P123 solution due to the fullerene-fullerene contacts between MMC_{60} molecules (Fig. 8a, d and g).[46] In 1% PVP solution, Y^{3+}-PyrHA shows fiber-like structure with the length of more than 10 μm (Fig. 8b), and the TEM image of Y^{3+}-PyrHA/MMC_{60} shows cluster–cluster aggregation (Fig. 8c). However, nanoparticles (10~60 nm) can be observed when Y^{3+}-PyrHA and Y^{3+}-PyrHA/MMC_{60} are dispersed in 1% F127 (Fig. 8e and f) or 1% P123 solution (Fig. 8h and i).

The TEM image of MMC_{70} shows irregular aggregates in 1% PVP solution (Fig. 9a), lamellar aggregates in 1% F127 (Fig. 9c) and cluster-cluster aggregation in 1% P123 solution (Fig. 9d), respectively. Similar to Y^{3+}-PyrHA/MMC_{60}, the TEM images of Y^{3+}-PyrHA/MMC_{70} show cluster–cluster aggregation in 1% PVP (Fig. 9b) and nanoparticles (10~ 60 nm) in 1% F127 (Fig. 9d) and 1% P123 solution (Fig. 9f).

Precipitation would be obtained when the buffer solution of Y^{3+}-PyrHA (50 μM) containing 1% PVP is subject to high speed centrifugation (> 10,000 rpm). However, the buffer solution of Y^{3+}-PyrHA (50 μM) containing 1% F127 or 1% P123

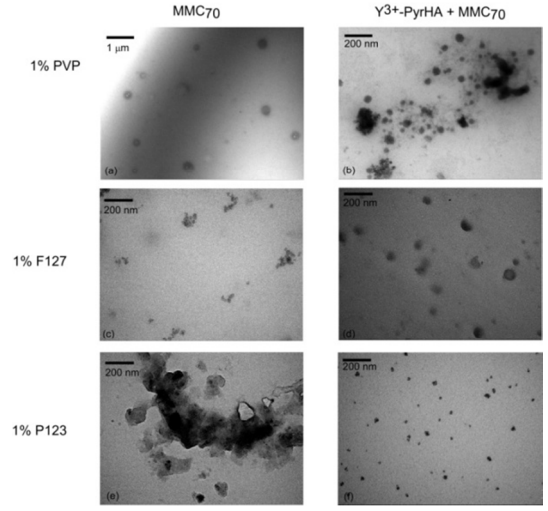

Fig. 9 TEM images of MMC_{70} (a, c, e) and Y^{3+}-PyrHA/MMC_{70} (b, d, f) in buffer solution (HEPES, 10 mM, pH 7.4) containing 1% PVP, 1% F127 and 1% P123. [MMC_{70}] = [Y^{3+}-PyrHA] = 50 μM.

remains clear after centrifugation and is stable for one month without precipitation at room temperature. It has been reported that PVP can form complex with drugs through hydrophobic interaction.[47] Considering that lanthanide ions possess a large coordination number (in the range of 6-12) on formation of a complex, the lanthanide ion (Y^{3+}) in Y^{3+}-PyrHA may chelate with the ether oxygen groups in F127 or P123 to saturate its coordination number.[48] As a result, the interaction between Y^{3+}-PyrHA and F127 or P123 is much stronger than that between Y^{3+}-PyrHA and PVP.

The interaction between amphiphilic polymer and Y^{3+}-PyrHA also plays an important role in controlling the size and morphology of Y^{3+}-PyrHA/fullerene. In 1% PVP solution, large size aggregates (> 200 nm) are observed for Y^{3+}-PyrHA/MMC_{60} and Y^{3+}-PyrHA/MMC_{70}, probably due to poor-dispersion of Y^{3+}-PyrHA. While in 1% F127 and 1% P123, the TEM images of Y^{3+}-PyrHA/fullerene shows nanoparticles (10~ 60 nm), probably due to good-dispersion of Y^{3+}-PyrHA, and these results suggest that the host-guest interaction is important for the morphology of supramolecular system.[49] As revealed by dynamic light scattering (DLS) results (Fig. S3), the hydrodynamic radius distributions *f*(Rh) of both Y^{3+}-PyrHA/MMC_{60} in P123 and Y^{3+}-PyrHA/MMC_{70} in P123 are narrowly dispersed in size, exhibiting an intensity-average hydrodynamic radius (Rh) of 109.7 nm (PDI = 0.173) and 83.4 nm (PDI = 0.255), respectively. This is in reasonable agreement with the size dimensions determined by TEM (Fig. 8 and 9). It is well known that the TEM technique determines nanoparticle dimensions in the dry state, whereas DLS reports intensity average dimensions in solution.[50]

Nanosecond Transient Absorption

Information on the dynamic excited–state interaction in Y^{3+}-PyrHA/fullerene is obtained by utilizing transient absorption spectra. No transient absorption signal is observed when Y^{3+}-PyrHA is irradiated with 355 nm laser in DMSO-toluene (4/1, v/v), maybe due to the very fast charge recombination of ion pair Y^{3+}-$Pyr^{\bullet+}HA^{\bullet-}$.[51] MMC_{60} presents characteristic triplet absorption

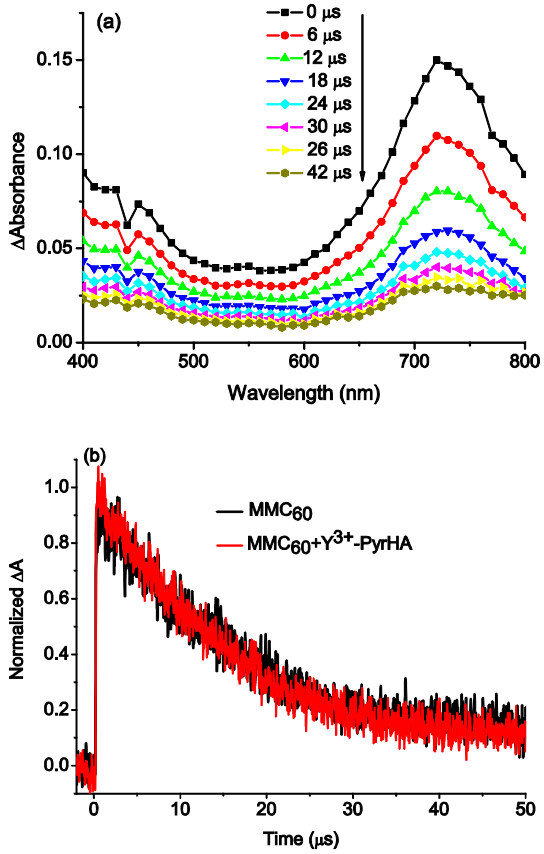

Fig. 10 (a) Transient absorption spectra of MMC_{60} (20 μM) observed by 355 nm laser irradiation in Ar-saturated DMSO-toluene (4/1, v/v). (b) Time profiles of MMC_{60} at 720 nm in the absence and presence of Y^{3+}-PyrHA in Ar-saturated DMSO-toluene (4/1, v/v) solution. [Y^{3+}-PyrHA] = [MMC_{60}] = 40 μM.

band with maximum around 720 nm (Fig. 10a). The decay curve for MMC_{60} at 720 nm can be fitted mono-exponentially with lifetime of 22.3 μs, in consistent with our previous study.[20] The lifetime of $^3MMC_{60}^*$ is not affected by Y^{3+}-PyrHA (Fig. 10b), suggesting that the interaction between triplet MMC_{60} and Y^{3+}-PyrHA is very weak. The absorption band of $MMC_{60}^{\bullet-}$ at 1020 nm cannot be detected, further indicating that photoinduced electron transfer between the pyrene group in Y^{3+}-PyrHA and MMC_{60} does not occur. These results demonstrate that the electron transfer is not the major pathway for the fluorescence quenching of pyrene moiety in Y^{3+}-PyrHA by MMC_{60} (Fig. 6 and 7).

The triplet lifetime of MMC_{60} is reduced to 8.84 μs when MMC_{60} dispersed in 1 % P123 aqueous solution in the presence and absence of Y^{3+}-PyrHA (Fig. S4). In air saturated DMSO-toluene (4/1, v/v) and 1% P123 buffer solution, the triplet lifetimes of MMC_{60} reduce to 0.73 and 0.53 μs, respectively (Fig. S5). That suggests energy transfer from the excited triplet state of MMC_{60} to the ground-state oxygen. No triplet signal of MMC_{60} could be detected in 1% PVP or in 1% F127 aqueous solution. Both P123 and F127 are amiphiphilic block copolymers and can encapsulate hydrophobic photosensitizers into the hydrophobic core.[52] However, P123 is more hydrophobic than F127,[53] providing different microenvironment and inducing different photophysical behaviour of MMC_{60}.[54] PVP may form a charge-

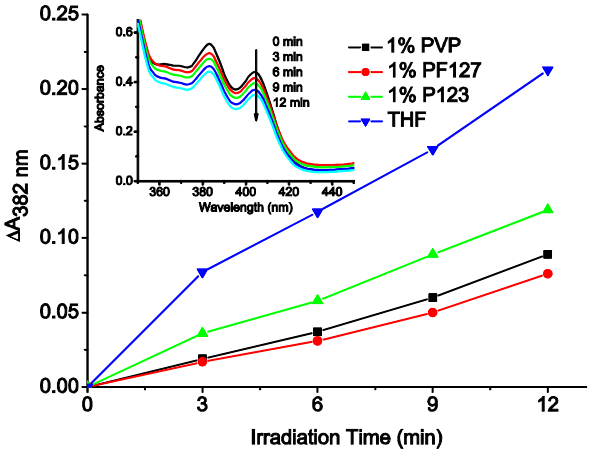

Fig. 11 MAS bleaching method for measuring the quantum yield of $^1O_2$ of MMC_{60} in THF and buffer solution containing 1% PVP, 1% F127 or 1% P123 irradiated with high-pressure mercury lamp (> 300 nm). Inset: absorption spectra of MAS bleaching system illuminated at 0, 3, 6, 9, 12 min in 1% P123 buffer solution (HEPES, 10 mM, pH 7.4). The arrow indicates the direction of changes. [MAS] = 80 μM, [MMC_{60}] = 5 μM.

Table 2 Relative quantum yields of $^1O_2$ for photosensitizers in 1% PVP, 1% F127and 1% P123 buffer solution[a,b]

[Y^{3+}-PyrHA] = [MMC_{60}] = [MMC_{70}] = 5 μM.

	1% PVP	1% F127	1% P123
MMC_{60}	0.41	0.35	0.56
MMC_{70}	0.32	0.35	1.05
Y^{3+}-PyrHA	0.51	0.35	0.69
Y^{3+}-PyrHA/MMC_{60}	0.43	0.38	0.84
Y^{3+}-PyrHA/MMC_{70}	0.42	0.37	1.33

[a]The $^1O_2$ generation quantum yield of MMC_{60} in THF solution is set to be unity. [b]All the samples are irradiated with high-pressure mercury lamp (> 300 nm).

transfer complex with fullerenes and the excited state of fullerene could be quenched by PVP.[55] When MMC_{70} dispersed in polymer solutions, including 1% PVP, 1% F127 and 1% P123 solution, no significant transient signals were detected, which can be attributed to the strong solvent-fullerene and fullerene-fullerene interactions.[56]

Relative quantum yields of singlet oxygen

Singlet oxygen ($^1O_2$) is one of the reactive intermediates in photodynamic therapy (PDT); consequently, the quantum yield of $^1O_2$ is an important parameter for the evaluation and optimization of the photosensitizer used in PDT. The photooxidation of MAS to its endoperoxide derivative by singlet oxygen is used to determine the quantum yield of $^1O_2$.[57,26] Fig. 11 shows the rates of MAS bleaching at 382 nm photosensitized by MMC_{60} in THF and amphiphilic polymer solution as a function of irradiation time.

Assuming $^1O_2$ generation quantum yield of MMC_{60} in THF solution to be unity, the relative quantum yields of $^1O_2$ for photosensitizers are summarized in Table 2. The relative $^1O_2$ quantum yields of MMC_{60} in polymer buffer solutions are much lower than that in THF due to aggregation of MMC_{60}. Longer triplet lifetime of MMC_{60} is favorable for higher quantum yield of $^1O_2$ (Fig. 10).[58] As a result, the quantum yield of $^1O_2$ for MMC_{60} in 1% P123 is higher than that in 1% PVP or 1% F127 (Fig. 11).

In Y^{3+}-PyrHA/MMC_{60} complex, both direct irradiation and energy transfer from photoexcited pyrene moieties in Y^{3+}-PyrHA to fullerene can lead to singlet excited state fullerene ^{1}MMC60* (Figure S2). The latter undergoes intersystem crossing (ISC) to give triplet excited state of fullerene $^3MMC_{60}$*. Singlet oxygen forms efficiently via triplet energy transfer from $^3MMC_{60}$* and triplet Y^{3+}-PyrHA. As a result, the $^1O_2$ quantum yield for Y^{3+}-PyrHA/fullerene is higher than that of Y^{3+}-PyrHA and MMC_{60} in P123 solution (Table 2).

In P123 solution, the $^1O_2$ quantum yield of MMC_{70} is higher than that of MMC_{60} (Table 2), in consistent with the reported results that $^1O_2$ quantum yield of C_{70} is higher than that of C_{60} under UV light irradiation in nonpolar solvent and micelle.[59] Similarly, the $^1O_2$ quantum yield for Y^{3+}-PyrHA, MMC_{70}, Y^{3+}-PyrHA/MMC_{60} and Y^{3+}-PyrHA/MMC_{70} in 1% P123, is also higher than that in 1% PVP or 1% F127 (Table 2). These results indicate that the composition and hydrophilic-hydrophobic balance of the amphiphilic polymer exert significant effect on the triplet excited states and consequently, on the singlet oxygen generating capacity of Y^{3+}-PyrHA, fullerene derivatives and their supramolecular assembly. The relative quantum yields of $^1O_2$ for Y^{3+}-PyrHA/fullerene is higher than that for Y^{3+}-PyrHA and the corresponding fullerene in 1% P123.

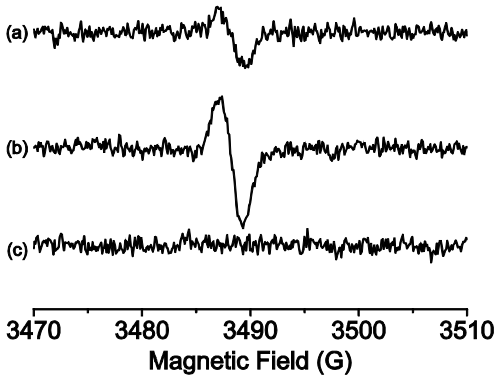

Fig. 12 (a) Photoinduced EPR spectrum of deoxygenated solution of Y^{3+}-PyrHA (20 μM) in DMSO-toluene (4/1, v/v) upon irradiation at 355 nm for 2 min. (b) Similar to (a), but with the addition of triethylamine (1 mM). (c) Similar to (a), but without irradiation.

EPR experiments

Irradiation of the Ar-saturated DMSO-toluene solution of Y^{3+}-PyrHA for 2 min at 355 nm, an EPR signal appears, with the same position and line shape as that of the radical anion of HA (Fig. 12a). A remarkable increase in intensity of EPR signal is observed when triethylamine, a strong electron donor, is added (Fig. 12b), and this observation further proves the assignment of this EPR signal to radical anion of HA. Control experiment confirms that light is necessary to produce this EPR signal (Fig. 12c). When the concentration of HA is high (0.1 mM), the

formation of radical anions of hypocrellins is the result of self-

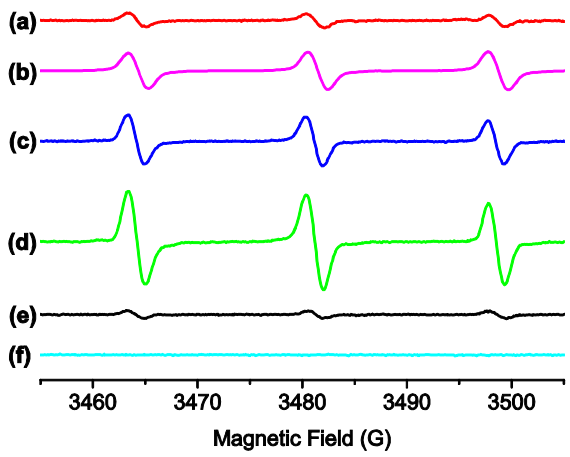

Fig. 13 EPR spectra of an air-saturated (a) 1% P123 buffer solution (HEPES, 10 mM, pH 7.4) and (b) THF solution of MMC_{60} containing TEMP (50 mM) after irradiated for 3 min upon laser irradiation (532 nm). (c) Similar to (a), but with Y^{3+}-PyrHA instead of MMC_{60}. (d) Similar to (a), but with addition of Y^{3+}-PyrHA. (e) Similar to (a), but in the presence of NaN_3 (1 mM). (f) Similar to (d) but without oxygen, TEMP or irradiation. [Y^{3+}-PyrHA] = [MMC_{60}] = 20 μM.

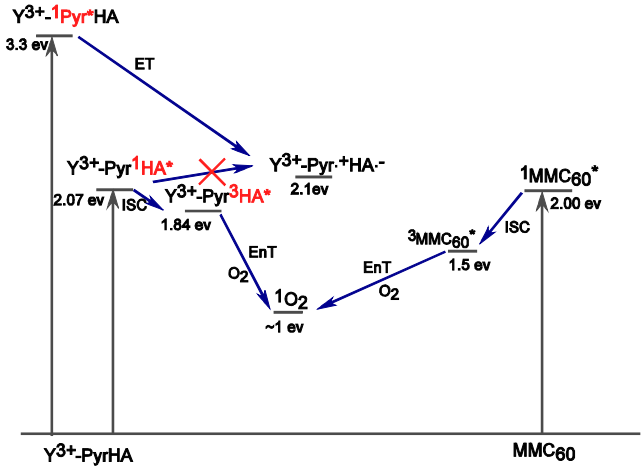

Fig. **14** Schematic energy diagrams in Y^{3+}-PyrHA/MMC_{60} system. ET and EnT mean electron transfer and energy transfer, respectively.

electron transfer between excited and ground state hypocrellin.[60] In the present study, relative low concentration of Y^{3+}-PyrHA (20 μM) is employed, and the EPR signal of radical anions HA mainly comes from photoinduced intramolecular electron transfer from the pyrene moiety to the HA moiety in Y^{3+}-PyrHA (eqn (3)). These results confirm that fluorescence of pyrene moiety in Y^{3+}-PyrHA is quenched by intramolecular electron transfer (Fig. 6).

Y^{3+}-^{1}Pyr*HA→Y^{3+}-Pyr•+$HA^{•-}$ (3)

The EPR spin trapping technique with 2,2,6,6-tetraethyl-4-piperridone (TEMP) as spin trapper is used to detect the formation of $^1O_2$. Irradiation of air-saturated 1% P123 solution of MMC_{60} (20 μM) and TEMP (50 mM) with a 532 nm laser yields a typical three-line EPR signal with the hyperfine coupling constant α^N = 16.0 G and g = 2.0056 (Fig. 13a), assigned to TEMPO, the adduct of $^1O_2$ and TEMP.[61] Compared to MMC_{60} in 1% P123, the TEMPO signal increases by about 2 times for MMC_{60} in air-saturated THF solution (Fig. 13b), in accordance with the results shown in Table 2. The TEMPO signal also can be observed when the 1% P123 solution of Y^{3+}-PyrHA and Y^{3+}-PyrHA/MMC_{60} are irradiated (Fig. 13c and d). When NaN_3, a typical $^1O_2$ scavenger, is present, the signal is suppressed efficiently (Fig. 13e). The signal in control experiments confirms that photosensitizers, oxygen, TEMP and light are all essential for the signal generation (Fig. 13f). The EPR signal intensity decreases in the following order: Y^{3+}-PyrHA/MMC_{60} in 1% P123> Y^{3+}-PyrHA in 1% P123> MMC_{60} in THF> MMC_{60} in 1% P123. The TEMPO signal generated by Y^{3+}-PyrHA/MMC_{60} is much stronger than that generated by Y^{3+}-PyrHA or MMC_{60} under the same condition, suggesting that the singlet oxygen generation capability can be enhanced by elaborate supramolecular assembly.[62]

The photodynamics in Y^{3+}-PyrHA/MMC_{60} complex is summarized in Fig.14. When Y^{3+}-PyrHA is irradiated with high pressure mercury lamp (> 300 nm), both pyrene and hypocrellin units can be excited. The photoinduced intramolecular electron transfer from excited pyrene unit to ground state hypocrellin unit is disadvantageous for the efficient generation of single oxygen,[63] which may explain why the relative quantum yields of $^1O_2$ for Y^{3+}-PyrHA and Y^{3+}-PyrHA/MMC_{60} in 1% P123 solution are lower than that for MMC_{60} in THF (Table 2).

However, when irradiated with a 532 nm laser, only the hypocrellin unit in Y^{3+}-PyrHA can be selectively excited. The intramolecular photoinduced electron transfer reaction from ground state of pyrene to singlet excited state of hypocrellin unit is thermodynamic unfavorable (ΔG = 0.16 eV), calculated by Rehm-Weller equation (eqn (2)), using oxidation potential of pyrene (1.25 V vs SCE),[37] first reduction potential of thiol substituted hypocrellin (-0.98 V vs SCE) and singlet state energy of hypocrellin (2.07 ev). [21] As a result, Y^{3+}-PyrHA and Y^{3+}-PyrHA/MMC_{60} in 1% P123 solution shows higher $^1O_2$ generation ability than that of MMC_{60} in THF solution with 532 nm laser irradiation (Fig. 13). In Y^{3+}-PyrHA/MMC_{60} complex, singlet oxygen forms efficiently via triplet energy transfer from $^3MMC_{60}$ and triplet Y^{3+}-PyrHA, and the aggregation of MMC_{60} can be remarkably reduced in Y^{3+}-PyrHA/MMC_{60} complex (Fig. 8). Therefore, the $^1O_2$ quantum yield for Y^{3+}-PyrHA/fullerene is higher than that of Y^{3+}-PyrHA and MMC_{60} in 1% P123 solution, respectively (Table 2 and Fig. 13).

Conclusions

In conclusion, Y^{3+} coordination polymer of pyrene modified HA (Y^{3+}-PyrHA) is synthesized, which can act as host for fullerene derivative MMC_{60} and MMC_{70}. The apparent 1:1 association constant between Y^{3+}-PyrHA and fullerene derivatives in amphiphilic polymer solution is higher than that in DMSO-toluene solution due to the microenvironment provided by amphiphilic polymer in aqueous solution. The composition and hydrophilic-hydrophobic balance of the amphiphilic polymer may influence the size, morphology and photophysical properties of Y^{3+}-PyrHA/fullerene assembly. Y^{3+}-PyrHA/fullerene exhibits narrow disperse in 1% P123 solution, and the quantum yields of $^1O_2$ for Y^{3+}-PyrHA/fullerene in 1% P123 solution is higher than that for Y^{3+}-PyrHA/fullerene in 1% P127 solution or 1% PVP solution.

Acknowledgment

This research is supported by National Natural Science Foundation of China (21073143), "Chunhui Project" from the Ministry of Education of China (NOs. Z2009-1-71002, Z2009-1-71006), NPU Foundation for Fundamental Research (JCY20130144, JC20100239), graduate starting seed fund of Northwestern Polytechnical University (Z2014171, Z2014172), NPU Foundation for Graduate Innovation.

Notes and references

[a] *The Key Laboratory of Space Applied Physics and Chemistry Ministry of Education, Department of Applied Chemistry, School of Science, Northwestern Polytechnical University, Xi'an, 710072, People's Republic of China. Fax& Tel: +86 29 88431677; E-mail: ouzhize@nwpu.edu.cn; gaoyunyan@nwpu.edu.cn*

[b] *CAS Key laboratory of Photochemistry, Institute of Chemistry, Chinese Academy of Sciences, Beijing 100190, People's Republic of China*

[c] *Technical Institute of Physics and Chemistry, Chinese Academy of Sciences, Beijing, 100190, People's Republic of China*

† Electronic Supplementary Information (ESI) available: supplementary MALDI-TOF mass spectrum of Y^{3+}-PyrHA, Fluorescence spectra of Y^{3+}-PyrHA/MMC_{60}, and transient absorption spectra of MMC_{60} in 1% P123 solution in the presence and absence of Y^{3+}-PyrHA. See DOI: 10.1039/b000000x/

1 A. M. Spokoyny, D. Kim, A. Sumrein and C. A. Mirkin, *Chem. Soc. Rev.*, 2009, **38**, 1218; N. R. Champness, *Angew. Chem. Int. Ed.*, 2009, **48**, 2274; W. J. Peard and R. T. Pflaum, *J. Am. Chem. Soc.*, 1958, **80**, 1593; F. W. Knobloch and W. H. Rauscher, *J. Polym. Sci.*, 1959, **38**, 261.

2 F. Novio, J. Simmchen, N. Vázquez-Mera, L. Amorín-Ferré and D. Ruiz-Molina, *Coord. Chem. Rev.*, 2013, **257**, 2839; N. Yanai and S. Granick, *Angew. Chem. Int. Ed.*, 2012, **51**, 5638; Y. C. Pan, D. Heryadi, F. Zhou, L. Zhao, G. Lestari, H. B. Su, and Z. P. Lai, *CrystEngComm*, 2011, **13**, 6937.

3 A. M. Spokoyny, D. Kim, A. Sumrein and C. A. Mirkin, *Chem. Soc. Rev.*, 2009, **38**, 1218; W. B. Lin, W. J. Rieter and K. M. L. Taylor, *Angew. Chem. Int. Ed.*, 2009, **48**, 650; A. Carne, C. Carbonell, I. Imaz and D. Maspoch, *Chem. Soc. Rev.*, 2011, **40**, 291; N. Stock and S. Biswas, *Chem. Rev.*, 2012, **112**, 933.

4 M. H. Zeng, Q. X. Wang, Y. X. Tan, S. Hu, H. X. Zhao, L. S. Long and M. Kurmoo, *J. Am. Chem. Soc.*, 2010, **132**, 2561.

5 I. Imaz, J. Hernando, D. Ruiz-Molina and D. Maspoch, *Angew. Chem.*, 2009, **121**, 2361; M. Oh and C. A. Mirkin, *Nature*, 2005, **438**, 651.

6 N. Yanai, T. Uemura, M. Inoue, R. Matsuda, T. Fukushima, M. Tsujimoto, S. Isoda and S. Kitagawa, *J. Am. Chem. Soc.*, 2012, **134**, 4501.

7 W. J. Rieter, K. M. Pott, K. M. L. Taylor and W. Lin, *J. Am. Chem. Soc.*, 2008, **130**, 1158; M. Pang, A. J. Cairns, Y. Liu, Y. Belmabkhout, H. C. Zeng and M. Eddaoudi, *J. Am. Chem. Soc.*, 2012, **134**, 13176; K. Liu, H. You, G. Jia, Y. Zheng, Y. Huang, Y. Song, M. Yang, L. Zhang and H. Zhang, *Cryst. Growth Des.*, 2010, **10**, 790.

8 Y. Yan, A. de Keizer, M. A. C. Stuart, M. Drechsler and N. A. M. Besseling, *J. Phys. Chem. B*, 2008, **112**, 10908; Y. Yan, L. Harnau, N. A. M. Besseling, A. de Keizer, M. Ballauff, S. Rosenfeldt and M. A. C. Stuar, *Soft Matter.*, 2008, **4**, 2207.

9 L. Xing, H. Zheng and S. Che, *Chem. Eur. J.*, 2011, **17**, 7271.

10 X. Shen, S. Wu, Y. Liua, K. Wang, Z. Xu and W. Liu, *J. Coll. Interf. Sci.*, 2009, **329**, 188.

11 E. Nakamura and H. Isobe, *Acc. Chem. Res.*, 2003, **36**, 807.

12 D. M. Guldi and M. Prato, *Acc. Chem. Res.*, 2000, **33**, 695; S. D. Snow, J. Lee and J. Kim, *Environ. Sci. Technol.*, 2012, **46**, 13227.

13 P. Mroz, G. P. Tegos, H. Gali, T. Wharton, T. Sarna and M. R. Hamblin, *Photochem. Photobiol. Sci.*, 2007, **6**, 1139.

14 S. Kim, D. J. Lee, D. S. Kwag, U. Y. Lee, Y. S. Youn and E. S. Lee, *Carbohydr. Polym.*, 2014, **101**, 692; J.-F. Nierengarten, J.-F. Eckert, Y. Rio, M. del Pilar Carreon, J.-L. Gallani and D. Guillon, *J. Am. Chem. Soc.*, 2001, **123**, 9743.

15 Y. Gao, Z. Ou, J. Chen, G. Yang, X. Wang, B. Zhang, M. Jin and L. Liu, *New J. Chem.*, 2008, **32**, 1555.

16 Y. Liu, Z. X. Yang, Y. Chen, Y. Song and N. Shao, *ACS Nano*, 2008, **2**, 554.

17 J. M. Napoles-Duarte, R. Lopez-Sandoval, A. Y. Gorbatchev, M. Reyes-Reyes and D. L. Carroll, *J. Phys. Chem. C*, 2009, **113**, 13677.

18 W. Jiang, B. Y. Kim, J. T. Rutka and W. C. Chan, *Nat. Nanotechnol.*, 2008, **3**,145.

19 S. Kim, D. J. Lee, D. S. Kwag, U. Y. Lee, Y. S. Youn and E. S. Lee, *Carbohydr. Polym.*, 2014, **101**, 692; M. Akiyama, A. Ikeda, T. Shintani, Y. Doi, J. Kikuchi, T. Ogawa, K. Yogo, T. Takeya and N. Yamamoto, *Org. Biomol. Chem.*, 2008, **6**, 1015.

20 E. Badamshina and M. Gafurova, *J. Mater. Chem.*, 2012, **22**, 9427; M. Raoofa, Y. Mackeyev, M. A. Cheney, L. J. Wilson and S. A. Curley, *Biomaterials*, 2012, **33**, 2952; N. Aich, L. K Boateng, J. R. V. Flora and N. B Saleh, *Nanotechnology*, 2013, **24**, 395602.

21 Z. Ou, H. Jin, Y. Gao, S. Li, H. Li, Y. Li, X. Wang and G. Yang, *J. Phys. Chem. B*, 2012, **116**, 2048; Z. Ou, C. Guo, Y. Gao, S. Li, W. Yin, Y. Li, M. Jin, X. Wang and G. Yang, *J. Photochem. Photobiol. A: Chem.*, 2011, **217**, 228.

22 K. Datta, M. Banerjee, B. K. Seal, A. K. Mukherjee, *J. Chem. Soc., Perkin Trans. 2*, 2000, 531.

23 R. C. Rowe, P. J. Sheskey and S. C. Owen, Handbook of Pharmaceutical Excipients, fifth ed., Pharmaceutical Press, Great Britain and American Pharmacists Association, Washington, 2006.

24 Y. I. Park, Y. Parka, J. Gao, J. K. Grey, C. Wang, M. A. Johal, J. Park, H. Y. Woo and H. Wang, *Polymer*, 2014, **55**, 855; M. C. Stuparu, *Angew. Chem. Int. Ed.*, 2013, **52**, 7786.

25 A. Pitto-Barry and N. P. E. Barry, *Polym. Chem.*, 2014, **5**, 3291

26 Y. Gao, Z. Wang, Z. Ou, Y. Li, X. Wang and G. Yang, *Chin. J. Chem.*, 2012, **30**, 418; H. Li, Y. Gao, Z. Ou, H. Jin, L. Cao and C. Chen, *Imag. Sci. Photochem.*, 2013, **31**, 197.

27 L. Zhang, J. Chen, S. Li, J. Chen, Y. Li, G. Yang and Y. Li, *J. Photochem. Photobiol. A: Chem.*, 2006, **181**, 429.

28 L. Stella, A. L. Capodilupo and M. Bietti, *Chem. Commun.*, 2008, 4744.

29 Y. Inoue, K. Yamamoto, T. Wada, S. Everitt, X. Gao, Z. Hou, L. Tong, S. Jiang and H. Wu, *J. Chem. Soc., Perkin Trans. 2*, 1998, 1807.

30 Y. Y. He, J. Y. An, W. Zou and L. J. Jiang, *J. Photochem. Photobiol. B: Photobiol.*, 1998, **44**, 45.

31 C. Adam, L. Garcia-Rio, J. R. Leis and J. A. Moreira, *Tetrahedron*, 2006, **62**, 8822.

32 T. Seko, M. Kato, H. Kohno, S. Ono, K. Hashimura, H. Takimizu, K. Nakai, H. Maegawa, N. Katsube and M. Toda, *Bioorg. Med. Chem. Lett.*, 2001, **11**, 2067.

33 A. E. Jr. Harvey and D. L. Manning, *J. Am. Chem. Soc.*, 1950, **72**, 4488.

34 Y. Rondelez, G. Bertho and O. Reinaud, *Angew. Chem. Int. Ed.*, 2002**,** **41**, 1044.

35 M. J. Rashkin and M. L. Waters, *J. Am. Chem. Soc.*, 2002, **124**, 1860.

36 Y. Gao, Z. Ou, Z. Zhang, S. Li, G. Yang and X. Wang, *Acta Phys. Chim. Sin.*, 2009, **25**,74.

37 H. Jaegfeldt, T. Kuwana and G. Johansson, *J. Am. Chem. Soc.*, 1983, **105**, 1805.

38 G. J. Kavarnos. Fundamentals of photoinduced electron transfer[M]. Wiley-VCH, John Wiley & Sons, Inc., New York, **1993**.

39 W. Yin, Z. Ou, Y. Gao, P. Hao, C. Guo, and Z. Wang, *Acta Chim. Sin.*, 2010, **14**, 1343.

40 F. Hauke, S. Atalick, D. M. Guldi, J. Mack, L. T. Scott and A. Hirsch, *Chem. Commun.*, 2004, 766; T. Gareis, O. Kothe and J. Daub, *Eur. J. Org. Chem.*,1998, 1549.

41 S. Bhattacharya, S. K. Nayak, S. Chattopadhyay, M. Banerjeea and A. K. Mukherjee, *Spectrochim. Acta, Part A*, 2002, **58**, 289.

42 T. Haino, Y. Matsumoto and Y. Fukazawa, *J. Am. Chem. Soc.*, 2005, **127**, 8936.

43 G. L. Martin, C. Lau, S. D. Minteer and M. J. Cooney, *Analyst*, 2010, **135**, 1131.

44 A. V. Kabanov, E. V. Batrakova and V. Y. Alakhov, *J. Control. Release*, 2002, **82**, 189.

45 B. Amina, R. Maxime and L. Jean-Christophe, *Pharm. Res.*, 2001, **18**, 323.

46 J. B. Hooper, D. Bedrov and G. D. Smith, *Langmuir*, 2008, **24**, 4550; S. Samal and K. E. Geckeler, *Chem. Commun.*, 2001, 2224.

47 H. A. Isakau, M. V. Parkhats, V. N. Knyukshto, B. M. Dzhagarov, E. P. Petrov and P. T. Petrov, *J. Photochem. Photobiol. B: Biol.*, 2008, **92**, 165.

48 R. D. Rogers, R. D. Etzenhouser, J. S. Murdoch and E. Reyes, *Inorg. Chem.*, 1991, **30**, 1445.

49 T. Fukushima, S. Horike, H. Kobayashi, M. Tsujimoto, S. Isoda, M. L. Foo, Y. Kubota, M. Takata and S. Kitagawa, *J. Am. Chem. Soc.*, 2012, **134**, 13341.

50 X. Hu, H. Li, S. Luo, T. Liu, Y. Jiang and S. Liu, *Polym. Chem.*, 2013, **4**, 695.

51 N. Mataga, H. Shioyama and Y. Kanda, *J. Phys. Chem.*, 1987, **91**, 314.

52 W. Li, X. Zhu, J. Wang, R. Liang, J. Li, S. Liu, G. Tu and J. Zhu, *J. Coll. Interf. Sci.*, 2014, **418**, 81.

53 T. M. Zhiyentayev, U. T. Boltaev, A. B. Solov'eva, N. A. Aksenova, N. N. Glagolev, A. V. Chernjak and N. S. Melik-Nubarov, *Photochem. Photobiol.*, 2014, **90**, 171.

54 L. Guo, B. Yan, J. Liu, K. Sheng and X. Wang, *Dalton Trans.*, 2011, **40**, 632.

55 C. Ungurenasu and A. Airinei, *J. Med. Chem.*, 2000, **43**, 3186.

56 Y. Rio, G. Accorsi, H. Nierengarten, J. Rehspringer, B. Honerlage, G. Kopitkovas, A. Chugreev, A. Van Dorsselaer, N. Armaroli and J. Nierengarten, *New J. Chem.*, 2002, **26**, 1146.

57 D. Arian, L. Kovbasyuk and A. Mokhir, *J. Am. Chem. Soc.*, 2011, **133**, 3972.

58 Z. Zeng, J. Zhou, Y. Zhang, R. Qiao, S. Xia, J. Chen, X. Wang and B. Zhang, *J. Phys. Chem. B*, 2007, **111**, 2688.

59 J. W. Arbogast and C. S. Foote, *J. Am. Chem. Soc.*, 1991, **113**, 8886.

60 Z. Ou, J. Chen, X. Wang, B. Zhang and Y. Cao, *New J. Chem.*, 2002, **26**, 1130.

61 Y. Lion, M. Delmelle and A. Van de Vorst, *Nature*, 1976, **263**, 442.

62 S. O. McDonnell, M. J. Hall, L. T. Allen, A. Byrne, W. M. Gallagher and D. F. O'Shea, *J. Am. Chem. Soc.*, 2005, **127**, 16360.

63 Z. Zeng, R. Qiao, J. Zhou, S. Xia, Y. Zhang, Y. Liu, J. Chen, X. Wang, B. Zhang, *J. Phys. Chem. B*, 2007, **111**, 3742.